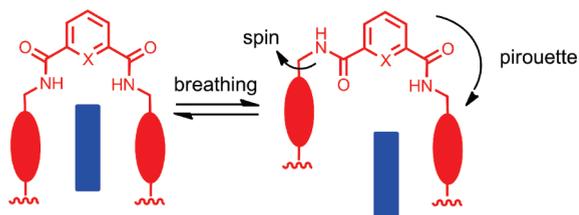# Macrocycle Breathing in [2]Rotaxanes with Tetralactam Macrocycles

Ivan Murgu, Jeffrey M. Baumes, Jens Eberhard,
Jeremiah J. Gassensmith, Easwaran Arunkumar, and
Bradley D. Smith*

*Department of Chemistry and Biochemistry, 236 Nieuwland
Science Hall, University of Notre Dame, Notre Dame,
Indiana 46556, United States*

smith.115@nd.edu

Received October 19, 2010

The structural dynamics of two pairs of [2]rotaxanes were compared using variable-temperature NMR. Each rotaxane had a surrounding tetralactam macrocycle with either 2,6-pyridine dicarboxamide or isophthalamide bridging units. Differences were observed in two types of rotational processes: spinning of the phenylene wall units in the surrounding macrocycle of squaraine rotaxanes and macrocycle pirouetting in xanthone rotaxanes. The rotaxanes with macrocycles containing 2,6-pyridine dicarboxamide bridges exhibited higher rotational barriers due to a cavity contraction effect, which disfavored macrocycle breathing.

Essentially all modern methods for preparing rotaxanes involve templated synthetic reactions, and in most cases the assembled product retains the noncovalent interactions that were the basis of the template effect.[1,2] The internally directed interactions, enforced by the mechanical bond, keep the interlocked components in close contact, restrict dynamic motion,[3] induce functional groups to adopt high-energy conformations,[4] and alter molecular reactivity.[5−7] In most cases the reactivity change is a decrease due to steric protection; however, we recently reported an unusual example of reaction acceleration. We discovered that the cyclor-eversion reaction of a tetralactam macrocycle containing an anthracene 9,10-endoperoxide group was increased substantially when the macrocycle encapsulated a squaraine thread component and thus existed as a [2]rotaxane.[5] Furthermore, large rate enhancements were obtained by making subtle changes in the structure of the two bridging units in the tetralactam macrocycle. For example, squaraine rotaxane macrocycles with bridging 2,6-pyridine dicarboxamide units were found to be 250 times more reactive than macrocycles with bridging isophthalamide units.[7a] While the influence of 2,6-pyridine dicarboxamide units on structural dynamics is well studied,[8] enhanced reactivity is a new molecular attribute that needs to be fully understood to ensure effective exploitation. Published X-ray crystal structures indicate that the 2,6-pyridine dicarboxamides contract the macrocycle cavity so that it wraps more tightly around the encapsulated squaraine thread.[7a,9] The driving force for this cavity contraction is formation of hydrogen bonds between the pyridyl nitrogen and the adjacent amide NH residues. This draws the

(1) For recent reviews of rotaxanes, see: (a) Hänni, K. D.; Leigh, D. A. *Chem. Soc. Rev.* **2010**, *39*, 1240–1251. (b) Ma, X.; Tian, H. *Chem. Soc. Rev.* **2010**, *39*, 70–80. (c) Harada, A.; Hashidzume, A.; Yamaguchi, H.; Takashima, Y. *Chem. Rev.* **2009**, *109*, 5974–6023. (d) Balzani, V.; Credi, A.; Venturi, M. *Chem. Soc. Rev.* **2009**, *38*, 1542–1550. (e) Stoddart, J. F. *Chem. Soc. Rev.* **2009**, *38*, 1802–1820. (f) Mullen, K. M.; Beer, P. D. *Chem. Soc. Rev.* **2009**, *38*, 1701–1713. (g) Loeb, S. J. *Chem. Soc. Rev.* **2007**, *36*, 226–235.

(2) For examples of rotaxane syntheses that eliminate the internally directed template interactions, see: (a) Aucagne, V.; Hänni, K. D.; Leigh, D. A.; Lusby, P. J.; Walker, D. B. *J. Am. Chem. Soc.* **2006**, *128*, 2186–2187. (b) Crowley, J. D; Goldup, S.; Lee, A. -L.; Leigh, D. A. *Chem. Soc. Rev.* **2009**, *38*, 1530–1541. (c) Leigh, D. A.; Lusby, P. J.; McBurney, R. T.; Symes, M. D. *Chem. Commun.* **2010**, *46*, 2382–2384. (d) Saito, S.; Takahashi, E.; Nakazono, K. *Org. Lett.* **2006**, *8*, 5133–5136.

(3) (a) Clegg, W.; Gimenez-Saiz, C.; Leigh, D. A.; Murphy, A.; Slawin, A. M. Z.; Teat, S. J. *J. Am. Chem. Soc.* **1999**, *121*, 4124–4129. (b) Yoon, I.; Miljanić, O. Š.; Benitez, D.; Khan, S. I.; Stoddart, J. F. *Chem. Commun.* **2008**, 4561–4563. (c) Miljanić, O. Š.; Dichtel, W. R.; Khan, S. I.; Mortezaei, S.; Heath, J. R.; Stoddart, J. F. *J. Am. Chem. Soc.* **2007**, *129*, 8236–8246. (d) Rijs, A. M.; Sändig, N; Blom, M. N.; Oomens, J.; Hannam, J. S.; Leigh, D. A.; Zerbetto, F.; Buma, W. J. *Angew. Chem., Int. Ed.* **2010**, *49*, 3896–3900. (e) Larsen, O. F. A.; Bodis, P.; Buma, W. J.; Hannam, J. S.; Leigh, D. A.; Woutersen, S. *Proc. Natl. Acad. Sci. U.S.A.* **2005**, *102*, 13378–13382. (f) Zhu, S. S.; Nieger, M.; Daniels, J.; Felder, T.; Kossev, I.; Schmidt, T.; Sokolowski, M.; Vögtle, F.; Schalley, C. A. *Chem.—Eur. J.* **2009**, *15*, 5040–5046. (g) Pons, M.; Millet, O. *Prog. Nucl. Magn. Reson. Spectrosc.* **2001**, *38*, 267–324. (h) Coutrot, F.; Busseron, E. *Chem.—Eur. J.* **2009**, *15*, 5186–5190. (i) Busseron, E.; Romuald, C.; Coutrot, F. *Chem.—Eur. J.* **2010**, *16*, 10062–10073. (j) Romuald, C.; Busseron, E.; Coutrot, F. *J. Org. Chem.* **2010**, *75*, 6516–6531. (k) Loeb, S. J.; Tiburcio, J.; Vella, S. J. *Chem. Commun.* **2006**, 1598–1600.

(4) (a) Leigh, D. A.; Lusby, P. J.; Slawin, A. M. Z.; Walker, D. B. *Angew. Chem., Int. Ed.* **2005**, *44*, 4557–4564. (b) Brancato, G.; Coutrot, F.; Leigh, D. A.; Murphy, A.; Wong, J. K. Y.; Zerbetto, F. *Proc. Natl. Acad. Sci. U.S.A.* **2002**, *99*, 4967–4971.

(5) Baumes, J. M.; Gassensmith, J. J.; Giblin, J.; Lee, J. -J.; White, A. G.; Culligan, W. J.; Leevy, W. M.; Kuno, M.; Smith, B. D. *Nature Chem.* **2010**, *2*, 1025–1030.

(6) For recent examples of steric protection, see: (a) Fernandes, A.; Viterisi, A.; Coutrot, F.; Potok, S.; Leigh, D. A.; Aucagne, V.; Papot, S. *Angew. Chem., Int. Ed.* **2009**, *48*, 6443–6447. (b) D'Souza, D. M.; Leigh, D. A.; Mottier, L.; Mullen, K. M.; Paolucci, F.; Teat, S. J.; Zhang, S. *J. Am. Chem. Soc.* **2010**, *132*, 9465–9470. (c) Gassensmith, J. J.; Matthys, S.; Lee, J. -J.; Wojcik, A.; Kamat, P. V.; Smith, B. D. *Chem.—Eur. J.* **2010**, *16*, 2916–2921.
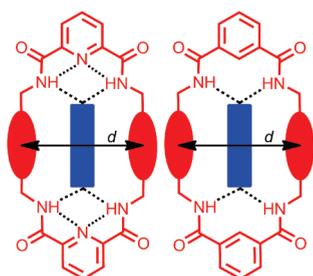
(7) (a) Baumes, J. M.; Murgu, I.; Oliver, A.; Smith, B. D. *Org. Lett.* **2010**, *12*, 4980–4983. (b) Gassensmith, J. J.; Baumes, J. M.; Eberhard, J.; Smith, B. D. *Chem. Commun.* **2009**, 2517–2519.

(8) See, for example: (a) Johnston, A. G.; Leigh, D. A.; Nezhat, L.; Smart, J. P.; Deegan, M. D. *Angew. Chem., Int. Ed. Engl.* **1995**, *34*, 1212–1216. (b) Schalley, C. A. *J. Phys. Org. Chem.* **2004**, *17*, 967–972. (c) Affeld, A.; Hübner, G. M.; Seel, C; Schalley, C. A. *Eur. J. Org. Chem.* **2001**, *25*, 2877–2890. and references therein.

(9) (a) Fu, N.; Baumes, J. M.; Arunkumar, E.; Noll, B. C.; Smith, B. D. *J. Org. Chem.* **2009**, *74*, 6462–6468. (b) Gassensmith, J. J.; Arunkumar, E.; Barr, L.; Baumes, J. M.; DiVittorio, K. M.; Johnson, J. R.; Noll, B. C.; Smith, B. D. *J. Am. Chem. Soc.* **2007**, *129*, 15054–15059. (c) Arunkumar, E.; Forbes, C. C.; Noll, B. C.; Smith, B. D. *J. Am. Chem. Soc.* **2005**, *127*, 3288–3289.

DOI: 10.1021/jo1020739

FIGURE 1. Schematic picture of [2]rotaxanes with red tetralactam macrocycle encapsulating blue thread component. X-ray structures of squaraine rotaxanes indicate that, when the macrocycle contains two 2,6-pyridine dicarboxamide units (left), $d = 6.61-6.78$ Å and when the macrocycle contains two isophthalamide units (right), $d = 6.91-7.18$ Å.[7a,9]

two cofacial aryl walls closer together as reflected by a shorter centroid-to-centroid distance d (Figure 1), and presumably induces molecular strain on an inward-directed endoperoxide.

While the solid-state evidence for macrocycle cavity contraction is quite compelling, we felt it necessary to confirm that the effect is maintained in solution. Therefore, we searched for NMR evidence of restricted conformational freedom in rotaxanes with surrounding tetralactam macrocycles containing bridging 2,6-pyridine dicarboxamide units. Here we report comparative studies of two pairs of unsymmetric rotaxane structures that were designed to produce inequivalent chemical shifts when certain types of conformational exchange processes became slow on the NMR time scale. The first process is spinning of the phenylene wall units in the surrounding macrocycle of squaraine rotaxanes **1** and **2** (Figure 2), and the second process is macrocycle pirouetting in rotaxanes **3** and **4** (Figure 3).[10] These segmental motions are diagnostic of a more global dynamic process that we call macrocycle breathing.[11] That is, stochastic expansion of the macrocyclic cavity due to bond vibration or dihedral rotation leads to weaker cross-component steric interactions in the rotaxane and opens up secondary pathways for other dynamic processes.

Unsymmetric squaraine rotaxanes **1** and **2** were prepared by standard Leigh-type clipping reactions using unsymmetric dye **5**.[12] Variable-temperature NMR studies of these compounds showed that spinning of the phenylene wall units was structure dependent. In rotaxane **2** (surrounding macrocycle with two bridging isophthalamide units), the chemical shift equivalence of protons designated as a and b in Figure 2 indicates that the two phenylene walls within the macrocycle spin rapidly compared to the 500 MHz NMR time scale, even at 223 K (Figure 4). In contrast, phenylene spinning in rotaxane **1** (surrounding macrocycle with two bridging 2, 6-pyridine dicarboxamide units) is considerably more hindered

(10) Previous studies of symmetric squaraine rotaxanes have shown that the surrounding macrocycle undergoes rapid interconversion between macrocyclic boat and chair conformations (see reference 9a). These structures had planar symmetry and thus did not allow observation of phenylene spinning and pirouetting motions by NMR. For an unusual example of a squaraine rotaxane with C_2 rotational symmetry that allowed observation of hindered bond rotations, see: Na, F.; Gassensmith, J. J.; Smith, B. D. *Aust. J. Chem.* **2010**, *63*, 792–796.

(11) The term *macrocycle breathing* is sometimes used in the literature to describe macrocycle vibrations that are observed in Raman spectroscopy.

(12) Gassensmith, J. J.; Baumes, J. M.; Smith, B. D. *Chem. Commun.* **2009**, 6329–6338.


5

1, X = N
2, X = CH
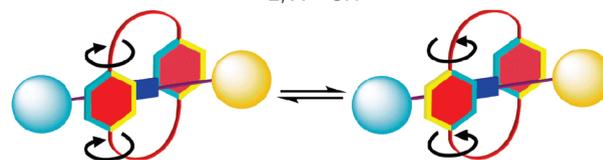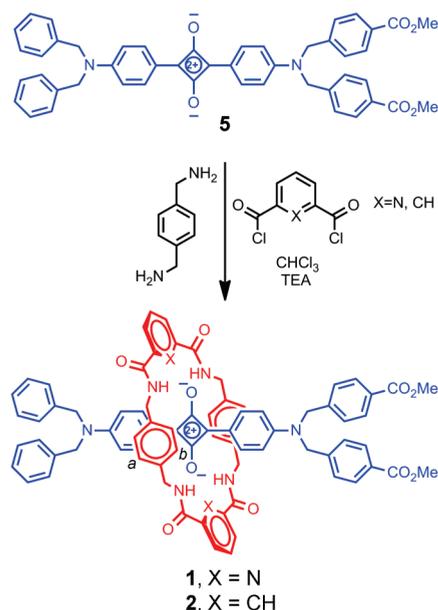
FIGURE 2. Spinning of phenylene wall units in squaraine rotaxanes **1** and **2**.

3 = 6 ⊃ 8
4 = 7 ⊃ 8

6, X = N, Y = H
7, X = CH, Y = *t*-Bu

8

$R = -(CH_2)_4-O-$
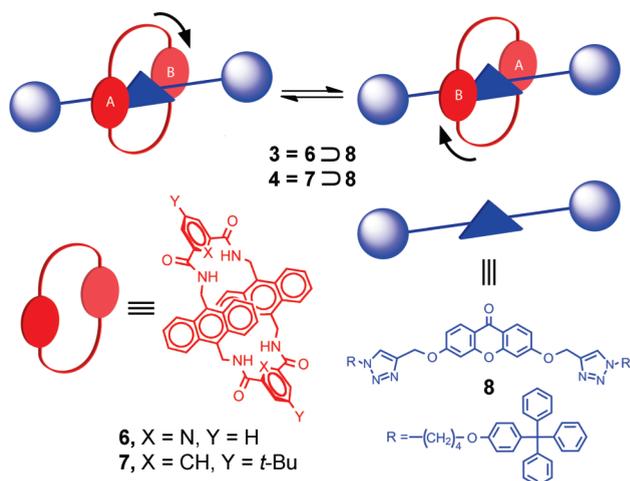
FIGURE 3. Macrocycle pirouetting in rotaxanes **3** and **4**.

such that protons a and b are inequivalent at room temperature. In weakly polar CDCl₃, the coalescence temperature for this two-site exchange was 306 K, which corresponds to an activation energy ($\Delta G^{\ddagger}$) of 15.4 kcal/mol. This was >4.8 kcal/mol higher than the barrier for phenylene-spinning in rotaxane **2** in CDCl₃. The activation energy decreased substantially with solvent polarity. For example, the spinning barrier for rotaxane **1** in CD₃CN, at 286 K, was 13.9 kcal/mol. It is also worth noting that addition of CD₃OD to a room temperature solution of **1** in CDCl₃ resulted in no time-dependent change in the ¹H NMR spectrum, whereas addition of CD₃OD to a solution of **2** induced complete proton−deuterium exchange at the amide residues within a few hours.
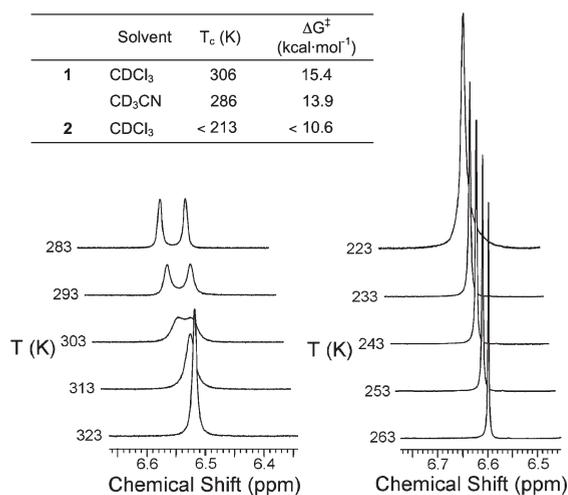
FIGURE 4. Selected variable-temperature ^{1}H NMR (500 MHz, CDCl$_3$) spectra of **1** (left) and **2** (right) showing peaks for protons *a* and *b*. Inset table shows the calculated activation energies ($\Delta G^\ddagger$) to phenylene spinning. Atom labeling in Figure 2.

SCHEME 1. **Synthesis of Xanthone Rotaxanes 3 and 4**

3, X = N, Y = H, 14 %
4, X = CH, Y = *t*-Bu, 26 %
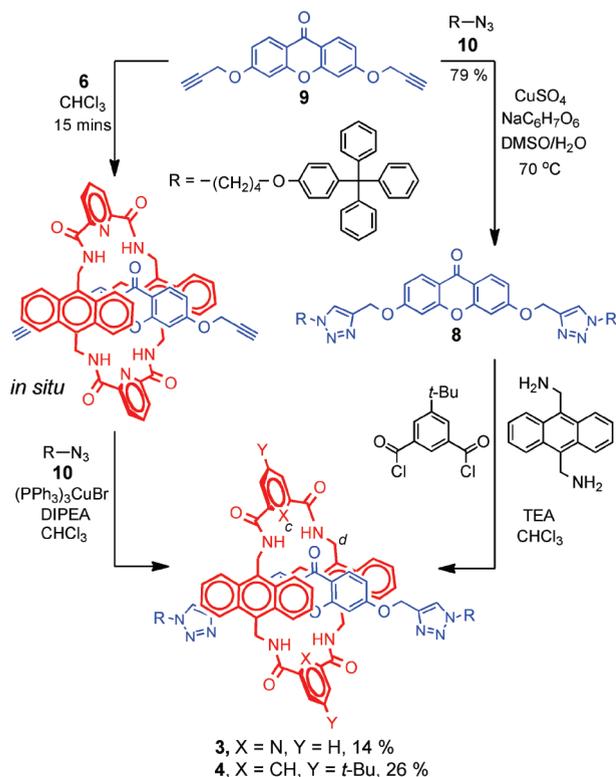
This suggests that the amide residues in **2** are more exposed to the surrounding solvent than in **1**.

3 and **4** (the second set of unsymmetric rotaxane structures) each has the same xanthone thread component, **8**, encapsulated inside the anthracene-containing macrocycles **6** and **7**, respectively. Both rotaxanes were prepared in modest yield by conducting templated synthesis reactions (Scheme 1). A clicked capping reaction was used to prepare **3**,[13]

(13) Gassensmith, J. J.; Barr, L.; Baumes, J. M.; Paek, A.; Nguyen, A.; Smith, B. D. *Org. Lett.* **2008**, *10*, 3343–3346.
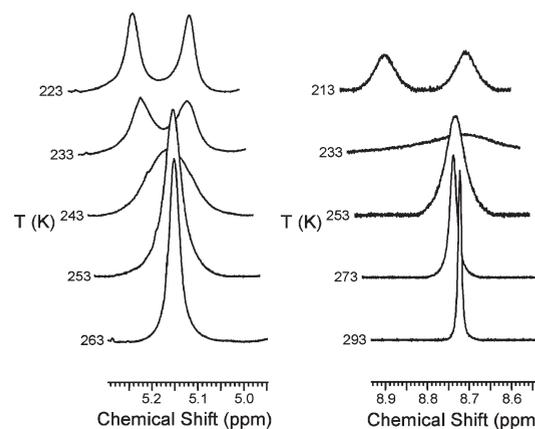
FIGURE 5. Variable-temperature ^{1}H NMR (500 MHz, CDCl$_3$) spectra of proton *d* in **3** (left) and proton *c* in **4** (right) exhibit coalescence temperatures of 241 and 233 K, respectively. Atom labeling in Scheme 1.

but this method was not successful in generating useful amounts of rotaxane **4**. Therefore, **4** was prepared by conducting a clipping reaction in the presence of xanthone thread component **8**. ^{1}H NMR spectra of both rotaxanes showed anisotropic shielding of chemical shifts due to the location of the tetralactam macrocycle over the core of the encapsulated xanthone thread, and also hydrogen bonding of the amide NH residues with the two different xanthone oxygen atoms. Variable-temperature NMR spectra of **3** and **4** indicated dynamic behavior (Figure 5). Structural assignment of the NMR signals that broadened and separated at low temperature showed unambiguously that the dynamic process was macrocycle pirouetting. As described in the Supporting Information, only peaks for the surrounding macrocycle split at low temperature, indicating a chemically inequivalent top and bottom. This implies a co-conformation with anisotropic shielding of the macrocycle by the unsymmetric core of the xanthone thread. In CDCl$_3$, the activation barriers for macrocycle pirouetting in rotaxanes **3** and **4** were determined to be 11.6 kcal/mol at 241 K and 10.6 kcal/mol at 233 K, respectively.

In both structural comparisons, the rotaxane with the surrounding macrocycle containing pyridine 2,6-dicarboxamide bridging units exhibited a higher rotational barrier. There is little doubt that the primary reason is internal hydrogen bonding of the pyridine nitrogen to adjacent amide NH residues, which produces two effects.[8] The first is to shorten the distance between the two cofacial aryl walls such that they stack more closely with the aromatic surfaces of the encapsulated thread (Figure 1). The second effect is to raise the activation barrier for macrocycle breathing. That is, single-bond rotation leads to flipping of an amide NH residue out of the macrocyclic cavity and transiently expands the cavity size (Figure 6).[14] Both of these effects could potentially explain the hindered phenylene spinning rate in **1** compared to that in **2** (Figure 2). However, phenylene spinning in **1** is accelerated substantially by changing to a more polar solvent, which leads us to conclude that macrocycle breathing is the dominant effect. The polar solvent stabilizes the transiently exposed NH residue that is part of conformation (b) in Figure 6. Macrocycle breath-

(14) A ROESY spectrum of rotaxane **2** in CDCl$_3$ at 40 °C produced no evidence that conformation (d) in Figure 6 is highly populated; thus, its lifetime is short and presumably even shorter in the case of rotaxane **1**.
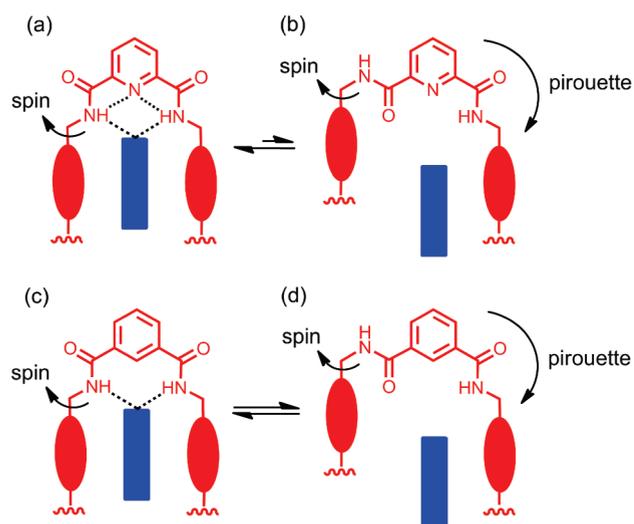
FIGURE 6. Macrocyclic breathing, which expands the cavity size and lowers the barrier for phenylene spinning and macrocycle pirouetting, is less favored when the rotaxane macrocycle contains two 2,6-pyridine dicarboxamide units (top equilibrium).

ing is also the best explanation for the difference in pirouetting rates for rotaxanes **3** and **4**. By definition, hydrogen bonds between the tetralactam macrocycle and the encapsulated thread must be broken during the pirouetting process. This is more likely to occur when the macrocycle cavity has expanded by adopting conformations (b) and (d). This breathing process is less favored when the macrocycle contains bridging 2, 6-pyridine dicarboxamides, i.e., the top equilibrium in Figure 6 lies to the left in weakly polar solvent.[8]

The solution-state dynamic NMR data in this study show clearly that rotaxanes with tetralactam macrocycles containing 2,6-pyridine dicarboxamides exhibit hindered segmental dynamics compared to analogous structures with bridging isophthalamides. This is consistent with the solid-state picture that rotaxane macrocycles containing 2,6-pyridine dicarboxamides are wrapped more tightly around the encapsulated thread and thus more likely to induce steric strain on functional groups that are constrained to be directed inward, toward the thread component (as in the case of squaraine rotaxane endoperoxides).[5,7] Macrocycle breathing is a cavity expansion event that provides access to low-energy pathways for secondary dynamic processes such as phenylene spinning and macrocycle pirouetting. This raises the idea of using intermolecular binding phenomena to control the breathing equilibrium and thus modulate either the rates of internal dynamic motion (machine-like behavior) or strain-induced chemiluminescent reactions (light-switching behavior).[15]

Experimental Section

General Synthesis of Rotaxanes 1−2, 4. Separate syringes were charged with solutions of the corresponding diacid chloride (1.0 mmol) in anhydrous chloroform (30 mL), and a mixture of the corresponding bis(amine) (1.0 mmol) and triethylamine (4.0 mmol) in anhydrous chloroform (30 mL). The two solutions were simultaneously added dropwise over 8 h (mechanical syringe pump) to a stirred solution containing the thread component (0.10 mmol) in anhydrous chloroform (20 mL). After stirring overnight, the reaction was filtered over Celite, concentrated, and

(15) Mullen, K. M.; Gunter, M. J. *J. Org. Chem.* **2008**, *73*, 3336–3350.

then purified by column chromatography using a column of silica gel with CHCl$_3$/MeOH (50:1) as the eluent. Spectral data for **1** (26%): ^{1}H NMR (500 MHz, CDCl$_3$) δ 3.94 (s, 6H), 4.38 (dd, *J* = 14.0 Hz, *J* = 5.5 Hz, 4H), 4.59 (dd, *J* = 14.0 Hz, *J* = 5.5 Hz, 4H), 4.64 (s, 4H), 4.74 (s, 4H), 6.17 (d, *J* = 9.5 Hz, 2H), 6.31 (d, *J* = 9.0 Hz, 2H), 6.55 (br d, 8H), 7.07 (d, *J* = 6.5 Hz, 4H), 7.21 (d, *J* = 8.5 Hz, 4H), 7.35−7.41 (m, 6H), 7.98 (t, *J* = 7.5 Hz, 2H), 8.06−8.08 (m, 6H), 8.10 (d, *J* = 9.5 Hz, 2H), 8.36 (d, *J* = 7.5 Hz, 4H), 9.83 (t, *J* = 5.5 Hz, 4H); ^{13}C NMR (125 MHz, CDCl$_3$) δ 29.7, 40.2, 43.2, 52.3, 54.4, 112.5, 119.8, 120.4, 123.7, 125.2, 126.4, 126.5, 128.1, 128.9, 129.2, 130.1, 130.5, 133.4, 134.2, 135.3, 136.8, 138.6, 140.8, 149.3, 154.2, 155.5, 163.4, 166.6, 184.7, 186.1, 188.0; MS (MALDI-TOF) calculated for C$_{78}$H$_{66}$N$_8$NaO$_{10}$ [M + Na]$^+$ 1297.5; found 1297.6.

Synthesis of Xanthone Rotaxane 3. Macrocycle **6** (24 mg, 0.032 mmol), bis-propargyl xanthone **9** (140 mg, 0.32 mmol), azide derivative **10** (140 mg, 0.32 mmol), tris(triphenylphosphine)copper(I) bromide (30 mg, 0.032 mmol), and diisopropylethylamine (8.3 mg, 0.064 mmol) were dissolved in chloroform (4 mL). The reaction mixture was stirred for 48 h at 50 °C, cooled to room temperature, and the solvent was evaporated. The reaction mixture residue was purified by column chromatography using silica gel with CHCl$_3$/MeOH (50:1) as eluent. Recrystallization from chloroform solution with diffusion of diethyl ether gave rotaxane **3** as a yellow solid (8.5 mg, 14%). ^{1}H NMR (600 MHz, CDCl$_3$) δ 1.84−1.90 (m, 4H), 2.16−2.22 (m, 4H), 4.00 (t, *J* = 6.0 Hz, 4H), 4.54 (t, *J* = 7.0 Hz, 4H), 4.90 (s, 4H), 5.19 (d, *J* = 4.0 Hz, 8H), 5.96 (dd, *J* = 9.0 Hz, *J* = 2.5 Hz, 2H), 6.30 (d, *J* = 2.5 Hz, 2H), 6.74 (d, *J* = 9.0 Hz, 4H), 6.86−6.93 (m, 8H), 7.10 (d, *J* = 9.0 Hz, 4H), 7.15 (d, *J* = 9.0 Hz, 4H), 7.16−7.25 (m, 30H), 7.52−7.59 (m, 8H), 7.72 (s, 2H), 8.22 (t, *J* = 8.0 Hz, 2H), 8.70 (d, *J* = 8.0 Hz, 4H), 8.80 (br s, 4H); ^{13}C NMR (150 MHz, CDCl$_3$) δ 26.3, 27.4, 37.4, 50.3, 61.6, 64.3, 66.7, 100.1, 111.8, 112.6, 113.1, 123.0, 124.2, 125.7, 125.8, 126.4, 127.4, 129.3, 129.7, 131.0, 132.2, 139.0, 139.3, 142.4, 146.9, 149.8, 154.1, 156.5, 162.2, 164.6, 175.5; HRMS (ESI) calculated for C$_{123}$H$_{101}$N$_{12}$O$_{10}$ [M + H]$^+$ 1905.7745; found 1905.7717.

Synthesis of Xanthone Thread 8. Bis-propargyl xanthone **9** (190 mg, 0.62 mmol), azide derivative **10** (580 mg, 1.3 mmol), copper(II) sulfate pentahydrate (190 mg, 0.76 mmol) and sodium ascorbate (250 mg, 0.12 mmol) were suspended in DMSO/water (40 mL, 9:1, v/v) and heated to 70 °C. After stirring for 64 h the suspension was cooled to room temperature and poured into chloroform/water (50 mL, 1:4, v/v). Brine and 0.1 M sodium ethylenediaminetetraacetate (Na$_4$EDTA) solution were added to improve phase separation; the organic phase was separated, and the greenish watery phase (CuEDTA) was extracted with chloroform (5 × 50 mL). The combined organic phase was washed with Na$_4$EDTA solution (0.1 M, 2 × 100 mL), water (2 × 200 mL), and finally with brine (100 mL). The colorless organic phase was dried with magnesium sulfate and filtered, and the solvent was removed under reduced pressure to give thread **8** as a white solid (480 mg, 79%). ^{1}H NMR (300 MHz, CDCl$_3$) δ 1.74−1.87 (m, 4H), 2.10−2.21 (m, 4H), 3.96 (t, *J* = 6.0 Hz, 4H), 4.48 (t, *J* = 7.0 Hz, 4H), 5.31 (s, 4H), 6.73 (d, *J* = 9.0 Hz, 4H), 6.97−7.02 (m, 4H), 7.10 (d, *J* = 9.0 Hz, 4H), 7.15−7.24 (m, 30H), 7.68 (s, 2H), 8.23 (d, *J* = 9.0 Hz, 2H); ^{13}C NMR (75 MHz, CDCl$_3$) δ 26.2, 27.3, 50.2, 62.4, 64.2, 66.7, 101.2, 113.1, 113.4, 116.1, 120.0, 123.0, 125.8, 127.4, 128.2, 131.0, 132.2, 139.2, 146.9, 156.5, 157.8, 163.0, 175.4; HRMS (FAB) calculated for C$_{77}$H$_{67}$N$_6$O$_6$ [M + H]$^+$ 1171.5117; found 1171.5136.

Supporting Information Available: Synthesis and spectral characterization, photophysical properties, dynamic NMR spectra, and rotational barrier calculations. This material is available free of charge via the Internet at http://pubs.acs.org.